Vibrational antiresonance in nonlinear coupled systems

Prasun Sarkar and Deb Shankar Ray*
Indian Association for the Cultivation of Science, Jadavpur, Kolkata-700032, India

(Received 22 January 2019; published 30 May 2019)

We examine the response of a system of coupled nonlinear oscillators driven by a rapidly varying field, to a low frequency weak periodic excitation of one of the oscillators. The response amplitude of the weak field-driven oscillator at an optimal strength of the rapidly varying field exhibits a strong suppression accompanied by a large negative shift in its oscillation phase. The minimum can be identified as vibrational antiresonance in between the two maxima corresponding to vibrational resonance. This vibrational antiresonance can be observed only in nonlinear coupled systems and not in linearly coupled systems or in a single nonlinear oscillator, under similar physical condition. We discuss the underlying dynamical mechanism, the role of nonlinearity and high frequency in characterizing this counter-resonance effect. Our theoretical analysis is corroborated by detailed numerical simulations.

DOI: 10.1103/PhysRevE.99.052221

I. INTRODUCTION

The response of a nonlinear system to a weak periodic signal in the presence of noise has been a topical theme in physical sciences since the 1980s. This phenomenon of stochastic resonance [1,2] and several of its variants have enriched our understanding of the constructive role of noise in weak signal amplification and in other issues, e.g., resonant activation [3,4], coherence resonance [5], noise-induced transition [6], wave propagation [7], pattern formation [8], to name a few. When the noise is replaced by a high frequency field one realizes vibrational resonance [9], i.e., the resonance enhancement of the response of the system to a weak periodic force at an optimal strength of the high frequency field. The numerical observation of this resonance phenomenon by Landa and McClintok [9] and subsequent theoretical [10] and experimental [11] investigations have paved the way for observation of several new high frequency field-induced effects [12,13]. Over the years, vibrational resonance along with other deterministic analogs of stochastic resonance have been the subject of a body of literature covering, e.g., ghost resonance [14], autoresonance [15], vibrational ratchets [16], nonlinear vibrational resonance [17], etc. We refer to [15] and Vincent *et al.* [18] for a comprehensive overview.

The focus of the present work is a theoretical and numerical analysis of an interesting, high frequency field-induced counter-resonance effect or antiresonance in a system of coupled nonlinear oscillators which has attracted little attention. To bring the issue in an appropriate perspective, we first revisit the aspect of antiresonance in the conventional [19] and some related [20,21] contexts. It is well known that when two or more linear oscillators are coupled and one of them is driven by a periodic field, the response of the driven oscillator displays antiresonance dips along with resonance maxima alternately in the response amplitude-frequency spectrum. Various features of the occurrence of antiresonance have been discussed in Chap. 14 of Ref. [15], in systems subjected to additive and multiplicative (parametric) periodic forces in the presence and absence of noise to demonstrate parametric antiresonance in coupled systems, stochastic antiresonance in single nonlinear oscillator, and conventional antiresonance in coupled Duffing systems. In Jothimurugan *et al.,* [19] conventional antiresonance and multiple resonance in coupled oscillators have been investigated in terms of amplitude of response vs frequency plot but in the absence of high frequency field. Vibrational resonance has been demonstrated in a single classical and quantum Morse oscillator [20], along with antiresonance in the quantum oscillator, shown by the variation of quantum transition probability with amplitude of the high frequency field. Single and multiple vibrational resonance in a quintic oscillator with monostable potential has also been discussed [21]. We now emphasize two points at this stage. First, an important hallmark of antiresonance is the large phase shift [22–26] in oscillation of one of the oscillators with respect to the other and is therefore is a characteristic feature of antiresonance which can occur in the coupled systems rather than a single oscillator, a point that has often been stressed in experiments [26] and engineering literature [22–24]. Notably this phase aspect is absent in these treatments which also lack any explicit analytic expression for amplitude or phase of the driven oscillator showing antiresonance *vis-à-vis* to that of the other oscillator(s), since the occurrence of antiresonance has been studied in a single oscillator [20,21]. Therefore this generic feature of the phase shift of one oscillator with respect to the other cannot arise. Second, the earlier studies on the system of coupled oscillators [15–19] focus on the conventional antiresonance or parametric antiresonance, where the high frequency modulation effect

*Corresponding author: pcdsr@iacs.res.in

is absent. The emphasis of the present work lies in the consideration of a high frequency field-induced antiresonance effect as a counterpart of vibrational resonance but in a system of coupled oscillators by taking care of the amplitude and phase response functions analytically and numerically for both the oscillators on an equal footing. The phenomenon can be observed only in nonlinear coupled systems but not in a single nonlinear oscillator or in coupled linear systems under similar physical conditions. This is the major point of departure from all the earlier treatments. Since antiresonance depends solely on the characteristics of the oscillator being driven, although coupled to others, in contrast to resonances which are dependent on all the component oscillators of the assembly, antiresonance has been useful for gaining information of the individual components. Its technical applications in electrical circuits [15,22], structural analysis [23], and mechanical engineering [24] are known. Antiresonance has also been demonstrated in an excitable biological system [25] and in a quantum system in the context of atom-cavity interaction in cavity electrodynamics [26] in the recent past.

The antiresonance in a coupled system of oscillators appears due to cancellation of the force acting via coupling to the undriven oscillators by the external drive acting directly on the single oscillator making the latter almost stationary. The question is whether this destructive interference can be optimized by the application of a high frequency field to each of the component oscillators after subsuming the field effect in the reduced dynamics as done in the treatment of vibrational resonance. The object of this paper is to address this question. In what follows, we consider a system of coupled bistable oscillators in the presence of high frequency field interacting with each of the components. The response of the system to a weak low frequency field is examined as a function of the strength of the high frequency field to show that the response amplitude of the low frequency driven oscillator exhibits a pronounced dip in between the vibrational resonance maxima. The dip corresponds to vibrational antiresonance which is accompanied by a large phase shift in its oscillation phase. This counter-resonance is conspicuously distinct by virtue of the following features: First, the signature of this antiresonance is marked on the response strength (of high frequency field) curve rather than on the response frequency (of low frequency drive) spectrum. Second, this vibrational antiresonance can occur only when the coupled system is nonlinear and one of the oscillators undergoes a large phase shift in its oscillation phase, in contrast to the conventional antiresonance which occurs even in linear systems [19]. We have explored the role of nonlinearity and high frequency field in characterizing this phenomenon. Detailed numerical simulations have been carried out to vindicate our theoretical scheme.

The paper is organized as follows: In Sec. II, we introduce a coupled nonlinear oscillator model for a theoretical analysis of vibrational antiresonance in terms of the expressions for the complex response functions for the oscillators. Section III is devoted to the detailed numerical simulations of the model. The paper is concluded in Sec. IV.

II. VIBRATIONAL ANTIRESONANCE IN COUPLED NONLINEAR SYSTEMS: THEORETICAL CONSIDERATIONS

A. Coupled nonlinear oscillator model

We begin with a model of linearly coupled nonlinear oscillators as governed by the following equations:

$$\ddot{x}_1 + 2\gamma_1\dot{x}_1 - 2g_1x_2 + \beta_1x_1^3 - \omega_1^2x_1 = 2F\cos\omega t + G\cos\Omega t \tag{2.1}$$

and

$$\ddot{x}_2 + 2\gamma_2\dot{x}_2 - 2g_2x_1 + \beta_2x_2^3 - \omega_2^2x_2 = G\cos\Omega t, \tag{2.2}$$

where γ_1 and γ_2 are the damping constants of the oscillators characterized by their phase space coordinates $(x_1, \dot{x_1})$ and $(x_2, \dot{x_2})$; g_1 and g_2 refer to the respective coupling coefficients. ω_1 and ω_2 are the linear coefficients and β_1 and β_2 represent the nonlinear coefficients, respectively. A low frequency signal having amplitude $2F$ and frequency ω is applied to the first oscillator for measuring the response. Each of the oscillators is perturbed by a high frequency field $G\cos\Omega t$. The frequency Ω is much higher compared to other frequencies of the system like ω_1, ω_2, ω. i.e., $\Omega \gg \omega, \omega_1, \omega_2$. In absence of the high frequency field $G\cos\Omega t$, the coupled system of equations, without or with nonlinearity, describes the conventional setup for antiresonance [19].

As the system is perturbed by a rapidly varying field, it is imperative that two time scales are associated with the dynamics. Provided the choice of relaxation scales set by γ_1, γ_2 and g_1, g_2 is appropriate and the rotating wave approximation is applicable so that one may neglect the fast counter-rotating terms over the time scale of interest, it is convenient to decompose the variables $x_1(t)$, $x_2(t)$ into slow parts $X_1(t, \omega t)$, $X_2(t, \omega t)$ and fast parts $\psi_1(t, \Omega t)$, $\psi_2(t, \Omega t)$, respectively, as done in vibrational mechanics [12–18] as

$$x_1(t) = X_1(t, \omega t) + \psi_1(t, \Omega t) \tag{2.3}$$

and

$$x_2(t) = X_2(t, \omega t) + \psi_2(t, \Omega t). \tag{2.4}$$

Here, ψ_1 and ψ_2 are 2π periodic and therefore have zero mean as

$$\langle\psi_i\rangle = \frac{1}{2\pi}\int_0^{2\pi}\psi_i(t, \tau)d\tau, \tag{2.5}$$

with $\tau = \Omega t$ and $i = 1, 2$ referring to the fast time scale. Substituting Eqs. (2.3) and (2.4) in Eqs. (2.1) and (2.2) and averaging over the fast time scale, we obtain the following equations for the slow moving component of motion for the first oscillator:

$$\ddot{X}_1 + 2\gamma_1\dot{X}_1 - 2g_1X_2 + \beta_1X_1^3 + 3\beta_1X_1^2\langle\psi_1\rangle - \omega_{1c}^2X_1 = 2F\cos\omega t, \tag{2.6}$$

and for the fast component

$$\ddot{\psi}_1 + 2\gamma_1\dot{\psi}_1 - 2g_1\psi_2 + 3\beta_1X_1^2(\psi_1 - \langle\psi_1\rangle) + 3\beta_1X_1\left(\psi_1^2 - \langle\psi_1\rangle^2\right) + \beta_1\psi_1^3 - \omega_1^2\psi_1 = G\cos\Omega t,$$
$$\text{where} \quad \omega_{1c}^2 = \omega_1^2 - 3\beta_1\langle\psi_1^2\rangle. \tag{2.7}$$

Similarly, for the second oscillator, we have

$$\ddot{X}_2 + 2\gamma_2\dot{X}_2 - 2g_2X_1 + \beta_2X_2^3 + 3\beta_2X_2^2\langle\psi_2\rangle - \omega_{2c}^2X_2 = 0, \tag{2.8}$$

and the fast component for the second oscillator takes the following form:

$$\ddot{\psi}_2 + 2\gamma_2\dot{\psi}_2 - 2g_2\psi_1 + 3\beta_2X_2^2(\psi_2 - \langle\psi_2\rangle) + 3\beta_2X_2\left(\psi_2^2 - \langle\psi_2\rangle^2\right) + \beta_2\psi_2^3 - \omega_2^2\psi_2 = G\cos\Omega t,$$
$$\text{where} \quad \omega_{2c}^2 = \omega_2^2 - 3\beta_2\langle\psi_2^2\rangle. \tag{2.9}$$

As ψ_1 and ψ_2 vary over a fast time scale, we assume further $\ddot{\psi}_i, \dot{\psi}_i \gg \psi_i, \psi_i^2, \psi_i^3$, etc. The dynamics of ψ_i $(i = 1, 2)$ is then given by

$$\ddot{\psi}_i + 2\gamma_i\dot{\psi}_i = G\cos\Omega t. \tag{2.10}$$

The solutions are

$$\psi_i = \frac{1}{2\gamma_i[1 + (\Omega/2\gamma_i)^2]}\left(\frac{G}{\Omega}\sin\Omega t - \frac{G}{2\gamma_i}\cos\Omega t\right),$$

so that $\langle\psi_i\rangle = 0$,

$$\langle\psi_i^2\rangle = \frac{G^2}{2}\left[\frac{1 + (2\gamma_i/\Omega)^2}{[(2\gamma_i)^2 + \Omega^2]^2}\right],$$

and $\langle\psi_i^3\rangle = 0$, for $i = 1, 2$. It is important to point out at this juncture that in our approach based on vibrational resonance literature, the high frequency perturbation adds up to the linear frequency term. Its average effect can be taken into consideration more effectively as in Ref. [27] for calculation of response of the slowly operated devices or for calculation of mobility [28].

Let us now consider the steady states X_{is}. These are $X_{is} = 0$ and $X_{is} = \pm\sqrt{\omega_{ic}^2/\beta_i}$, where the subscript s refers to the steady state and $i = 1, 2$. Thus the position of the fixed point can be controlled by G/Ω ratio. Linearization of the dynamics around the nontrivial steady state can be performed by expressing the small perturbation Y_i as $Y_i = (X_i - X_{is})$. This yields

$$\ddot{Y}_1 + 2\gamma_1\dot{Y}_1 - 2g_1Y_2 + \Omega_1^2Y_1 + \left(\beta_1X_{1s}^3 - 2g_1X_{2s} - \omega_{1c}^2X_{1s}\right) = 2F\cos\omega t, \tag{2.11}$$

and

$$\ddot{Y}_2 + 2\gamma_2\dot{Y}_2 - 2g_2Y_1 + \Omega_2^2Y_2 + \left(\beta_2X_{2s}^3 - 2g_2X_{1s} - \omega_{2c}^2X_{2s}\right) = 0, \tag{2.12}$$

where

$$\Omega_1^2 = \left(3\beta_1X_{1s}^2 - \omega_{1c}^2\right) = 2\omega_{1c}^2$$

and

$$\Omega_2^2 = \left(3\beta_2X_{2s}^2 - \omega_{2c}^2\right) = 2\omega_{2c}^2.$$

Ω_1 and Ω_2 are the effective strong field-dressed linear frequencies for the two oscillators. The contribution due to high frequency field has thus been incorporated in the resultant dynamics. In what follows we explore the response of this system to the low frequency field, $2F\cos\omega t$.

B. Vibrational antiresonance: Expressions for response amplitude and phase

We first use the following transformations to change the real variables $(Y_1, \dot{Y}_1)$ and $(Y_2, \dot{Y}_2)$ to the complex variables α_1 and α_2, such that

$$\alpha_1 = -\Omega_1Y_1 + i\dot{Y}_1 \tag{2.13}$$

and

$$\alpha_2 = -\Omega_2Y_2 + i\dot{Y}_2. \tag{2.14}$$

Equations (2.11) and (2.12) can then be written as two first order equations as follows:

$$\dot{\alpha_1} = i\Omega_1\alpha_1 - \gamma_1(\alpha_1 - \alpha_1^*) - i(\alpha_2 + \alpha_2^*)g_1/\Omega_2 + iF(e^{i\omega t} + e^{-i\omega t}) - iM_1, \tag{2.15}$$

and

$$\dot{\alpha_2} = i\Omega_2\alpha_2 - \gamma_2(\alpha_2 - \alpha_2^*) - i(\alpha_1 + \alpha_1^*)g_2/\Omega_1 - iM_2, \tag{2.16}$$

where

$$M_1 = \left(\beta_1X_{1s}^3 - 2g_1X_{2s} - \omega_{1c}^2X_{1s}\right)$$

and

$$M_2 = \left(\beta_2X_{2s}^3 - 2g_2X_{1s} - \omega_{2c}^2X_{2s}\right).$$

Transforming these equations to a frame which is rotating at the driving frequency $\alpha_i \to \alpha_ie^{i\omega t}$, we take the resort of rotating wave approximation and neglect the fast counter-rotating terms which are proportional to $e^{2i\omega t}$ and vanish on averaging over the time scale of interest as $(\omega + \Omega_i) \gg (\omega - \Omega_i)$. This yields

$$\dot{\alpha_1} = i(\Delta_1 + i\gamma_1)\alpha_1 + ig_1\alpha_2/\Omega_2 + iF, \tag{2.17}$$

and

$$\dot{\alpha_2} = i(\Delta_2 + i\gamma_2)\alpha_2 + ig_2\alpha_1/\Omega_1, \tag{2.18}$$

where Δ_i refer to detunings, $\Delta_i = (\omega - \Omega_i)$ between the slow drive and the effective frequencies. In the absence of damping, driving, or coupling, the solutions to these equations can be taken as

$$\alpha_i(t) = \alpha_i(0)e^{i\Delta_it}.$$

This represents a rotation in the complex α_i plane with the angular frequency Δ_i. The steady-state solutions for Eqs. (2.17) and (2.18) can be found by setting

$$\dot{\alpha_1} = \dot{\alpha_2} = 0.$$

These conditions yield the complex response functions for the oscillators as

$$\alpha_{1\text{steady}} = \frac{-F(\Delta_2 + i\gamma_2)}{\left[(\Delta_1 + i\gamma_1)(\Delta_2 + i\gamma_2) - \frac{g_1g_2}{\Omega_1\Omega_2}\right]} \tag{2.19}$$

and

$$\alpha_{2\text{steady}} = \frac{-F(g_2/\Omega_1)}{\left[(\Delta_1 + i\gamma_1)(\Delta_2 + i\gamma_2) - \frac{g_1g_2}{\Omega_1\Omega_2}\right]}. \tag{2.20}$$

Equations (2.19) and (2.20) are the theoretical expressions for the steady state response functions of the two oscillators and

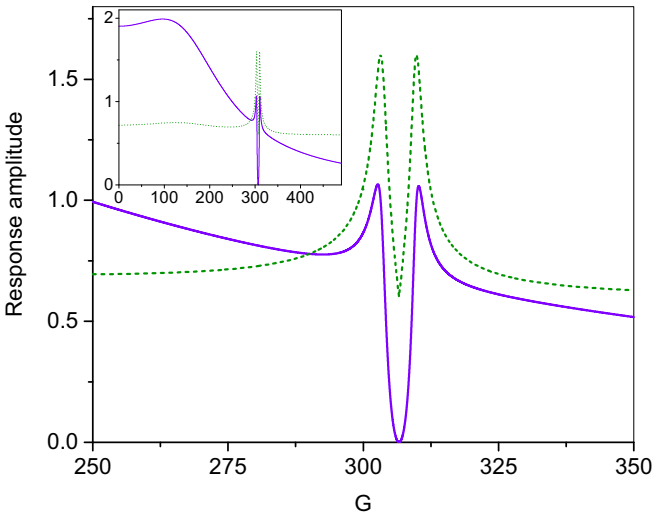

FIG. 1. The response amplitude for the oscillators (first oscillator: solid line; second oscillator: dotted line) calculated theoretically [Eqs. (2.19) and (2.20)] as a function of G, the strength of rapidly varying field for the set of parameters $\Omega = 10.0$, $\gamma_1 = \gamma_2 = 0.5$, $g_1 = g_2 = 0.05$, $\beta_1 = \beta_2 = 0.1$, displaying antiresonance minimum in between two vibrational maxima for the first oscillator. The inset depicts the variation for a wider range of G values (units arbitrary).

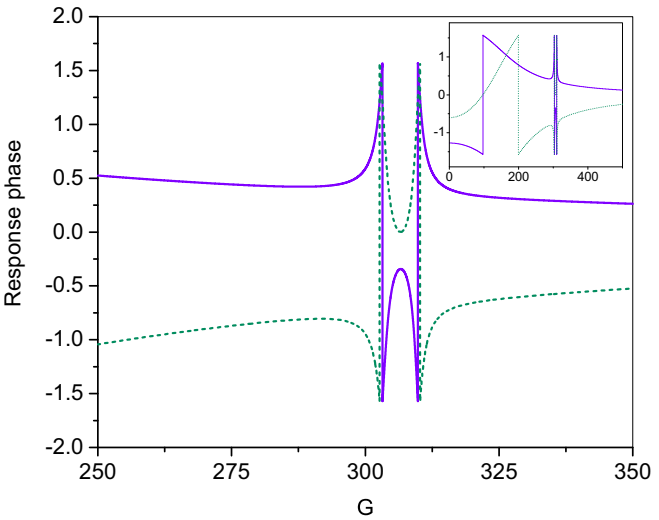

FIG. 2. The phase of the response function for the oscillators (first oscillator: solid line; second oscillator: dotted line) calculated theoretically [Eqs. (2.19) and (2.20)] as a function of G, the strength of rapidly varying field for the set of parameters mentioned in Fig. 1, displaying a negative phase shift for the first oscillator. The inset shows the variation of phase for a wider range of G values (units arbitrary).

constitute the main results of this section. In the following, we discuss some of their notable features, in terms of their amplitude and phase.

(i) A closer look at the detunings Δ_1 and Δ_2 clearly reveals that because of the dependence of Δ_i on the strength of the rapidly varying field G ($\Delta_i = \omega - \sqrt{2}\{\omega_i^2 - \frac{3\beta_i G^2}{2}[\frac{1+(2\gamma_i/\Omega)^2}{[(2\gamma_i)^2+\Omega^2]^2}]\}^{1/2}$) both the oscillators display resonances in the response amplitudes when G is varied. These can be identified as the vibrational resonances as shown in Fig. 1. In addition, the weakly driven oscillator denoted by the solid curve shows a pronounced dip for a $G_{\min}$ in between the two vibrational resonance maxima. The dip corresponds to antiresonance arising out of destructive interference of the weak driving force acting on the first oscillator and its interaction with the second one. The second oscillator, on the other hand, being undriven by weak force, remains in an almost quiescent state in this region as evident from the dotted curve in Fig. 1. The inset in Fig. 1 depicts the variation for a wider range of G values. Because of the dependence of the response amplitude on the strength of the high frequency field (G) the pronounced minimum in the response curve may be termed as "vibrational antiresonance" in analogy to vibrational resonance. The caveat, however, is that this antiresonance can be realized only in coupled nonlinear systems.

(ii) A conspicuous feature of antiresonance is a large phase shift. In Fig. 2, we exhibit the variation of phase of the two oscillators by solid (first oscillator) and dotted (second oscillator) curves as a function of the strength of the strong field (G) to demonstrate this phase shift. The inset depicts the variation of phase for a wider range of G values. As there is no analog of this phase shift in vibrational resonance, we emphasize that this variation of phase with the strength of high frequency field is a hallmark of this vibrational antiresonance.

(iii) Finally, we mention two distinctive features of the antiresonance as reflected in the response function: First, it is evident that vibrational resonances and antiresonance appear alternately in the response amplitude profile of the weakly driven oscillator, while the undriven oscillator displays no antiresonance. Second, as in the case of conventional antiresonance, the vibrational antiresonance observed for the system is found to be independent of the properties of the driven oscillator, i.e., it remains insensitive to the variation of resonance frequency or damping coefficient of the driven oscillator.

III. NUMERICAL SIMULATIONS

In order to confirm our theoretical observations based on perturbation analysis, we have carried out numerical simulations of the governing equations for the coupled nonlinear systems, Eqs. (2.1) and (2.2). For the present investigation we fix the parameter set as follows: $\omega_1 = \omega_2 = 1.1$, $\gamma_1 = \gamma_2 = 0.5$, $\beta_1 = \beta_2 = 0.1$, $g_1 = g_2 = 0.05$, $\omega = 1.4$, and $F = 1.0$. The strength G and frequency Ω of the high frequency field $G\cos\Omega t$ are used as the control parameters for the study of of the variation of the linear response amplitude and phase. The linear response of the ith oscillator of the coupled system is evaluated as usual, by numerically estimating the sine and cosine components $B_s^{(i)}(\omega)$ and $B_c^{(i)}(\omega)$, respectively, of the corresponding output signal $x_i(t)$ as follows:

$$B_s^{(i)}(\omega) = \frac{2}{\pi T}\int_0^{nT} x_i(t)\sin\omega t, \tag{3.1}$$

$$B_c^{(i)}(\omega) = \frac{2}{\pi T}\int_0^{nT} x_i(t)\cos\omega t, \tag{3.2}$$

where $T = 2\pi/\omega$ with integer n, ω being the frequency of the weak field $2F\cos\omega t$. Solving numerically Eqs. (2.1) and

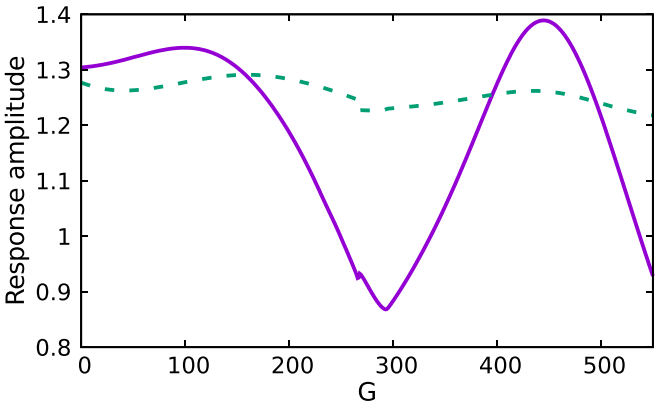

FIG. 3. The response amplitude for the oscillators (first oscillator: solid line; second oscillator: dotted line) calculated numerically using Eq. (3.3) as a function of G, the strength of rapidly varying field for the set of parameters mentioned in Fig. 1, displaying antiresonance minimum in between two vibrational maxima for the first oscillator (units arbitrary).

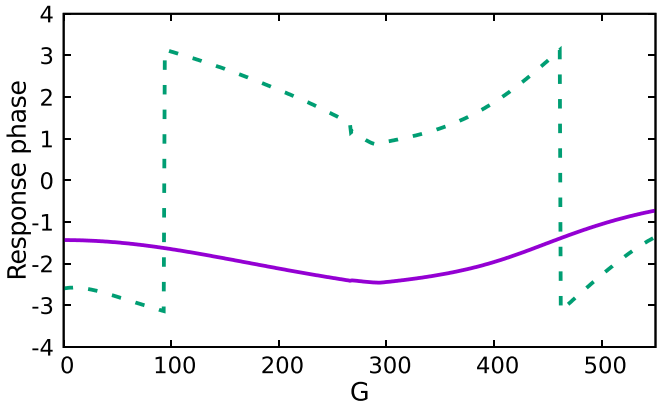

FIG. 4. The phase of the response function for the oscillators (first oscillator: solid line; second oscillator: dotted line) calculated numerically Eq. (3.4) as a function of G, the strength of rapidly varying field for the set of parameters mentioned in Fig. 1, displaying a negative phase shift for the first oscillator (units arbitrary).

(2.2) for $x_1(t)$ and $x_2(t)$ followed by evaluation of the sine and cosine components for the two oscillators, one obtains the amplitude of the response function

$$\alpha^{(i)}(\omega) = \sqrt{\left[B_s^{(i)}(\omega)\right]^2 + \left[B_c^{(i)}(\omega)\right]^2}/F, \tag{3.3}$$

and the phase shift

$$\theta^{(i)}(\omega) = \tan^{-1}\left[B_s^{(i)}(\omega)/B_c^{(i)}(\omega)\right], \tag{3.4}$$

for the response function of the ith oscillator. In Fig. 3, we depict the variation of the response function for the weakly driven and for the undriven oscillators by continuous and dotted curves, respectively, with the strength of high frequency force G for the aforesaid parameter values. It is evident that the vibrational antiresonance appears in between the two maxima corresponding to vibrational resonances for an optimal value of G for the driven oscillator. The antiresonance dip is absent for the undriven oscillator. We observe a qualitative agreement between the theoretical and numerical values of $G_{\min}$ for the position of antiresonance dip. The variation of oscillation phase of the driven and undriven oscillators with G is shown in Fig. 4. The large phase shift calculated numerically clearly corresponds qualitatively to that for the theoretically calculated value. However, there are some disagreements regarding the shape of the profiles. To be precise, theoretical profiles for the amplitude (Fig. 1) and the phase (Fig. 2) appear sharper compared to the corresponding numerically simulated profiles (Figs. 3 and 4). This may be understood as follows. Since the numerical simulation of the dynamics of the coupled nonlinear systems involves multiple frequencies, the required destructive interference between the coupling and the weak forcing is not complete because of these frequencies resulting in broadening of the profile of the response function. Our theoretical scheme on the other hand relies on two distinct time scales and an effective linearized slow dynamics around the steady state based on Eqs. (2.12) and (2.13) after elimination of fast variables. The width of the antiresonance dip therefore appears to be narrower and the corresponding variation of phase is sharper in the theoretical profiles as compared to those for the numerical ones. Furthermore, a little step adjacent to $G_{\min}$ appears in the numerical simulation in Fig. 3. This is absent in the corresponding analytical profile for the linearized version. Our numerical experience reveals that this step almost vanishes when the nonlinear coefficient β is raised to a high value, say to 0.2 for the present parameter set. A possible reason may be that for relatively high β, the nonlinear oscillators destructively interfere with the high frequency field in a more effective way, giving rise to a smooth profile. The discrepancies notwithstanding, the observation of vibrational antiresonance from theoretical calculations and numerical simulations appears as a phenomenon that reflects the constructive role of high frequency field. Finally, we mention that we have assumed equal coupling coefficients $g_1 = g_2$. A numerical scrutiny reveals that a disparity in the values of coupling coefficients does not affect the position of $G_{\min}$; only a little difference in the relative amplitude of the vibrational resonance maxima is observed.

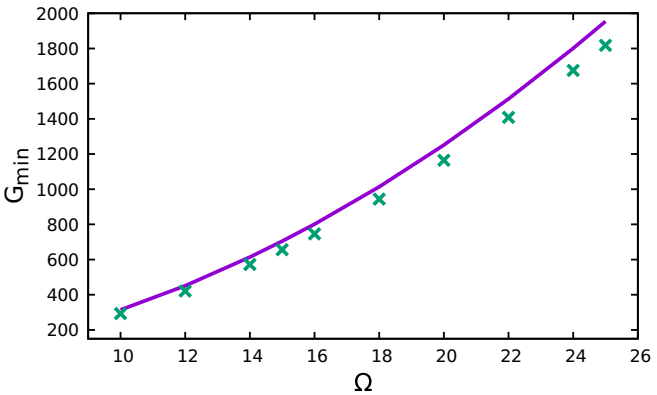

FIG. 5. The variation of antiresonance minimum for the first oscillator, calculated by numerical simulations (×) as a function of Ω, the frequency of the rapidly varying field for the parameter set $\gamma_1 = \gamma_2 = 0.5$, $g_1 = g_2 = 0.05$, $\beta_1 = \beta_2 = 0.1$. The continuous line represents the theoretical curve (units arbitrary).

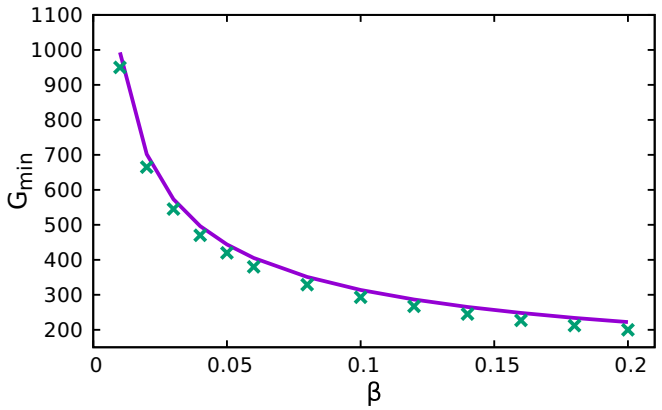

FIG. 6. The variation of antiresonance minimum for the first oscillator calculated by numerical simulations (×) as a function of β ($\beta_1 = \beta_2 = \beta$), the nonlinear coefficient for the parameter set: $\gamma_1 = \gamma_2 = 0.5$, $g_1 = g_2 = 0.05$, $\Omega = 10.0$. The continuous line represents the theoretical curve (units arbitrary).

Although the conventional antiresonance remains insensitive to the variation of the driven system parameters like damping coefficient or response frequency, the position of vibrational antiresonance minimum depends on the high frequency field $G\cos\Omega t$. This is because the effective linear frequency Ω_i depends on G/Ω ratio. In Fig. 5, we depict the variation of $G_{\min}$ as a function of the high frequency Ω as calculated numerically (denoted by crosses ×). The numerical simulation is based on estimation of $G_{\min}$ from the variation of the amplitude of the response function $\alpha^{(1)}(\omega)$ according to Eq. (3.3) as a function of G, for a given value of Ω. The procedure is repeated for several values of Ω while all other parameters are kept fixed. The continuous curve represents the corresponding theoretical variation of $G_{\min}$. The agreement is found to be excellent. Finally, we note that a crucial element in the phenomenon of vibrational antiresonance concerns nonlinearity generating multiple frequencies in the dynamics. The high frequency field effectively interferes with them so that the effective coupled dynamics follows a linearized dynamics around a steady state on a slow time scale. It is therefore likely that the nonlinearity of the dynamics would affect antiresonance. In Fig. 6, we illustrate the numerical variation of $G_{\min}$ as a function of the nonlinear parameter $\beta(=\beta_1 = \beta_2$ as denoted by crosses) and compared with the theoretical curve (denoted by a continuous line) for the same set of parameters. It is evident that the antiresonance dip appears for lower values of strength of the high frequency field for higher nonlinearity. The theoretical curve is found to be in good agreement with numerics.

IV. CONCLUSION

In this paper we have demonstrated a high frequency field-induced counter-resonance phenomenon corresponding to vibrational resonance. In contrast to conventional antiresonance as observed in a single nonlinear system or in coupled linear systems, this vibrational antiresonance accompanied by a large phase shift occurs only in a system of coupled nonlinear oscillators each of which, in addition, is driven by a high frequency field and the response of the weak-field-driven oscillator is optimized for an appropriate choice of amplitude of the high frequency field. While vibrational resonance depends on the properties of all the component oscillators of the coupled system as well as the coupling strength, vibrational antiresonance depends solely on the weakly driven oscillator. The position of this vibrational antiresonance dip is dependent on the high frequency of the strong field, similar to that for vibrational resonance. In real systems antiresonance is traditionally used for characterization of individual components in multicomponent systems. Our analysis of antiresonance in a minimal model of a pair of coupled bistable oscillators, based on the equations of slow motion, supported by direct numerical simulations can be extended to an array of nonlinear bistable, multistable, or excitable systems, to capture the essential characteristics of individual components. Two distinct dynamical mechanisms are apparent. First, the rapidly varying field interferes with various high frequencies due to the inherent nonlinearity of the system on a fast time scale. This leads us to the effective dynamics on a slow time scale. On the other hand, the low frequency drive acting on the oscillator destructively interferes with the coupling to the other oscillator on a slow time scale. This results in antiresonance. Keeping in view the two underlying time scales in the dynamics, the system parameters can be suitably manipulated to enhance, suppress, or modulate the antiresonance dip by taming the strong field. Because of the simplicity of the model, we believe that this vibrational antiresonance in coupled nonlinear systems is amenable to experimental verification using suitably designed electronic circuits.

ACKNOWLEDGMENTS

Thanks are due to the Science and Engineering Research Board, the Department of Science and Technology, Government of India, for a J. C. Bose National Fellowship, under Grant No. SB/ S2/JCB-030/2015, for partial financial support.

[1] R. Benzi, A. Sutera, and A. Vulpiani, J. Phys. A: Math. Gen. **14**, L453 (1981); S. Fauve and F. Heslot, Phys. Lett. A **97**, 5 (1983); B. McNamara, K. Wiesenfeld, and R. Roy, Phys. Rev. Lett. **60**, 2626 (1988).

[2] L. Gammaitoni, F. Marchesoni, E. Menichella-Saetta, and S. Santucci, Phys. Rev. Lett. **62**, 349 (1989); V. I. Melnikov, Phys. Rev. E **48**, 2481 (1993); L. Gammaitoni, P. Hänggi, P. Jung, and F. Marchesoni, Rev. Mod. Phys. **70**, 223 (1998); G. P. Harmer and B. R. Davis, IEEE Trans. Instrum. Meas. **51**, 299 (2002).

[3] C. R. Doering and J. C. Gadoua, Phys. Rev. Lett. **69**, 2318 (1992); M. Marchi, F. Marchesoni, L. Gammaitoni, E. Menichella-Saetta, and S. Santucci, Phys. Rev. E **54**, 3479 (1996); R. N. Mantegna and B. Spagnolo, Phys. Rev. Lett. **84**, 3025 (2000).

[4] P. K. Ghosh and D. S. Ray, J. Chem. Phys. **125**, 124102 (2006); A. Fiasconaro and B. Spagnolo, Phys. Rev. E **83**, 041122 (2011).

[5] A. S. Pikovsky and J. Kurths, Phys. Rev. Lett. **78**, 775 (1997); D. E. Postnov, S. K. Han, T. G. Yim, and O. V. Sosnovtseva, Phys. Rev. E **59**, R3791(R) (1999); G. Giacomelli, M. Giudici, S. Balle, and J. R. Tredicce, Phys. Rev. Lett. **84**, 3298 (2000); K. Miyakawa and H. Isikawa, Phys. Rev. E **66**, 046204 (2002).

[6] W. Horsthemke and R. Lefever, Phys. Lett. A **64**, 19 (1977); C. Van den Broeck, J. M. R. Parrondo, and R. Toral, Phys. Rev. Lett. **73**, 3395 (1994); P. K. Ghosh, D. Barik, and D. S. Ray, Phys. Lett. A **342**, 12 (2005).

[7] S. Alonso, I. Sendiña-Nadal, V. Pérez-Muñuzuri, J. M. Sancho, and F. Sagués, Phys. Rev. Lett. **87**, 078302 (2001).

[8] A. Sanz-Anchelergues, A. M. Zhabotinsky, I. R. Epstein, and A. P. Muñuzuri, Phys. Rev. E **63**, 056124 (2001); S. S. Riaz, S. Dutta, S. Kar, and D. S. Ray, Eur. Phys. J. B **47**, 255 (2005); S. Dutta, S. S. Riaz, and D. S. Ray, Phys. Rev. E **71**, 036216 (2005); D. Das and D. S. Ray, *ibid.* **87**, 062924 (2013); B. Spagnolo and A. La Barbera, Physica A **315**, 114 (2002); F. Sagués, J. M. Sancho, and J. García-Ojalvo, Rev. Mod. Phys. **79**, 829 (2007).

[9] P. S. Landa and P. V. E. McClintock, J. Phys. A: Math. Gen. **33**, L433 (2000).

[10] M. Gitterman, J. Phys. A: Math. Gen. **34**, L355 (2001); A. A. Zaikin, L. Lopez, J. P. Baltanás, J. Kurths, and M. A. F. Sanjuán, Phys. Rev. E **66**, 011106 (2002); I. I. Blekhman and P. S. Landa, Int. J. Nonlin. Mech. **39**, 421 (2004).

[11] V. N. Chizhevsky, E. Smeu, and G. Giacomelli, Phys. Rev. Lett. **91**, 220602 (2003)

[12] J. P. Baltanás, L. López, I. I. Blechman, P. S. Landa, A. Zaikin, J. Kurths, and M. A. F. Sanjuán, Phys. Rev. E **67**, 066119 (2003).

[13] C. Jeevarathinam, S. Rajasekar, and M. A. F. Sanjuán, Phys. Rev. E **83**, 066205 (2011); J. H. Yang and H. Zhu, Chaos **22**, 013112 (2012); Y. M. Qin, J. Wang, C. Men, B. Deng, and X. L. Wei, *ibid.* **21**, 023133 (2011); J. Shi, C. Huang, T. Dong, and X. Zhang, Phys. Biol. **7**, 036006 (2010).

[14] S. Rajamani, S. Rajasekar, and M. A. F. Sanjuán, Commun. Nonlin. Sci. Numer. Simulat. **19**, 4003 (2014).

[15] S. Rajasekar and M. A. F. Sanjuán, *Nonlinear Resonances*, Springer Series in Synergetics (Springer, Basel, Switzerland, 2016).

[16] M. Borromeo and F. Marchesoni, Phys. Rev. E **73**, 016142 (2006).

[17] S. Ghosh and D. S. Ray, Phys. Rev. E **88**, 042904 (2013); D. Das and D. S. Ray, Eur. Phys. J. B **91**, 279 (2018); V. N. Chizhevsky, Phys. Rev. E **90**, 042924 (2014).

[18] U. E. Vincent, T. O. Roy-Layinde, O. O. Popoola, P. O. Adesina, and P. V. E. McClintock, Phys. Rev. E **98**, 062203 (2018).

[19] S. Belbasi, M. E. Foulaadvand, and Y. S. Joe, Am. J. Phys. **82**, 32 (2014); R. Jothimurugan, K. Thamilmaran, S. Rajasekar, and M. A. F. Sanjuán, Nonlin. Dyn. **83**, 1803 (2015).

[20] K. Abirami, S. Rajasekar, and M. A. F. Sanjuán, Pramana J. Phys. **81**, 127 (2013).

[21] S. Jeyakumari, V. Chinnathambi, S. Rajasekar, and M. A. F. Sanjuán, Phys. Rev. E **80**, 046608 (2009).

[22] A. F. McKinley, T. P. White, I. S. Maksymov, and K. R. Catchpole, J. Appl. Phys. **112**, 094911 (2012); S. Lin and J. Xu, Sensors **17**, 329 (2017).

[23] F. Wahl, G. Schmidt, and L. Forrai, J. Sound Vib. **219**, 379 (1999).

[24] P. Sjövall and T. Abrahamsson, Mech. Syst. Signal Process. **22**, 15 (2008).

[25] H. G. Rotstein, J. Comput. Neurosci. **43**, 35 (2017).

[26] C. Sames, H. Chibani, C. Hamsen, P. A. Altin, T. Wilk, and G. Rempe, Phys. Rev. Lett. **112**, 043601 (2014).

[27] M. Borromeo and F. Marchesoni, Europhys. Lett. **72**, 362 (2005).

[28] M. Borromeo and F. Marchesoni, Phys. Rev. Lett. **99**, 150605 (2007).